BMC Chemistry

RESEARCH

Open Access

Antiplasmodial potential of phytochemicals from *Citrus aurantifolia* peels: a comprehensive in vitro and in silico study

Abeer H. Elmaidomy[1*], Usama Ramadan Abdelmohsen[2,3*], Ahmed M. Sayed[4], Faisal H. Altemani[5], Naseh A. Algehainy[5], Denisa Soost[6], Thomas Paululat[6], Gerhard Bringmann[7*] and Esraa M. Mohamed[8]

Abstract

Phytochemical investigation of Key lime (*Citrus aurantifolia* L., F. Rutaceae) peels afforded six metabolites, known as methyl isolimonate acetate (1), limonin (2), luteolin (3), 3`-hydroxygenkwanin (4), myricetin (5), and europetin (6). The structures of the isolated compounds were assigned by 1D NMR. In the case of limonin (2), further 1- and 2D NMR experiments were done to further confirm the structure of this most active metabolite. The antiplasmodial properties of the obtained compounds against the pathogenic NF54 strain of *Plasmodium falciparum* were assessed in vitro. According to antiplasmodial screening, only limonin (2), luteolin (3), and myricetin (5) were effective (IC_{50} values of 0.2, 3.4, and 5.9 µM, respectively). We explored the antiplasmodial potential of phytochemicals from *C. aurantifolia* peels using a stepwise in silico-based analysis. We first identified the unique proteins of *P. falciparum* that have no homolog in the human proteome, and then performed inverse docking, $\Delta G_{Binding}$ calculation, and molecular dynamics simulation to predict the binding affinity and stability of the isolated compounds with these proteins. We found that limonin (2), luteolin (3), and myricetin (5) could interact with 20S a proteasome, choline kinase, and phosphocholine cytidylyltransferase, respectively, which are important enzymes for the survival and growth of the parasite. According to our findings, phytochemicals from *C. aurantifolia* peels can be considered as potential leads for the development of new safe and effective antiplasmodial agents.

Keywords *Citrus*, Key lime, Network pharmacology, In silico analysis

*Correspondence:
Abeer H. Elmaidomy
Abeer011150@pharm.bsu.edu.eg
Usama Ramadan Abdelmohsen
usama.ramadan@mu.edu.eg
Gerhard Bringmann
bringman@chemie.uni-wuerzburg.de;
gerhard.bringmann@uni-wuerzburg.de
[1]Department of Pharmacognosy, Faculty of Pharmacy, Beni-Suef University, Beni-Suef 62514, Egypt
[2]Department of Pharmacognosy, Faculty of Pharmacy, Minia University, Minia 61519, Egypt
[3]Department of Pharmacognosy, Faculty of Pharmacy, Deraya University, Minia 61111, Egypt
[4]Department of Pharmacognosy, Faculty of Pharmacy, Nahda University, Beni-Suef 62513, Egypt
[5]Department of Medical Laboratory Technology, Faculty of Applied Medical Sciences, University of Tabuk, Tabuk 71491, Saudi Arabia
[6]Department of Chemistry and Biology, University of Siegen, Adolf-Reichwein-Str. 2, 57068 Siegen, Germany
[7]Institute of Organic Chemistry, University of Würzburg, Am Hubland, 97074 Würzburg, Germany
[8]Department of Pharmacognosy, Faculty of Pharmacy, MUST, Giza 12566, Egypt

Introduction

Malaria continues to be a serious threat to public health, particularly in tropical and subtropical countries. It is a disease caused by parasites belonging to several species of the genus *Plasmodium*, including *Plasmodium falciparum, P. malariae, P. ovale, P. vivax, and P. knowlesi*, which are spread via the bite of an infected female *Anopheles mosquito* [1]. The most virulent of these species is *P. falciparum*, it is responsible for the greatest levels of morbidity and mortality. It is, moreover, the most common species in sub-Saharan Africa (SSA), having the greatest rate of malaria infections and fatalities worldwide [1]. Globally in 2018, there were an estimated 249 million malaria cases and 608 000 malaria deaths in 85 countries. The World Health Organization WHO African Region carries a disproportionately high share of the global malaria burden. In 2018, the Region was home to 94% of malaria cases (233 million) and 95% (580 000) of malaria deaths. Children under 5 accounted for about 80% of all malaria deaths in the Region [1].

Chemotherapy can be used to treat malaria, although the parasites can be highly resistant against many of the medications. In 2006, Cambodia reported the first case of artemisinin resistance, which afterwards spread to the majority of South-East Asia [2]. Another key worry is the safety of chemoprophylaxis; for example, primaquine, atovaquone, and doxycycline are not recommended for use in young children and pregnant women [3]. All these issues make the development of new malaria medications necessary.

Natural substances, such as plant products, have significantly contributed to the development of new drugs during the past 50 years and have been of benefit to the pharmaceutical industry [4]. For instance, numerous pharmacological classes that were first developed based on active chemicals from plant sources have enabled therapies for different infectious diseases, cancer, and other debilitating diseases caused by metabolic abnormalities [4]. Additionally, the first components of antimalarial chemotherapy, quinine and artemisinin, as well as their synthetic analogs, were also derived from plant sources. Many people in malaria-endemic regions, particularly in Africa, turn to herbal remedies as the primary form of therapy [5]. The expense of conventional medications, accessibility, perceived efficacy, lack of adverse effects, and faith in traditional remedies are only some few of the frequent factors that influence people's preferences [6].

Citrus aurantifolia was imported to North Africa, Europe, and other parts of the world after being native to tropical and subtropical regions of Southeast Asia, including India and China [7]. It is also known as Key lime [8]. *C. aurantifolia* contains active phytochemical substances such as flavonoids including apigenin, hesperetin, kaempferol, nobiletin, quercetin, naringenin, and rutin [9, 10], as well as flavones [11], flavanones [12, 13] triterpenoids [14], and limonoids [15]. The traditional uses of *C. aurantifolia* from several literature reviews are described as antibacterial [16], antidiabetic [17], antifungal [18], antihypertensive [19], anti-inflammatory [20], anti-hyperlipidemic [21], anti-parasitic [22], and antiplatelet activities [11]. It is furthermore used for the treatment of cardiovascular [23], hepatic [24], osteoporosis [25], and urolithiasis disorders [26], and acts as a fertility promoter [27]. Moreover, it can be used for insecticidal activity [28].

Herein, we subjected the peels of *C. aurantifolia* to a stepwise chromatographic isolation to get information about the major phytochemicals in this waste product. Subsequently, we investigated whether the identified phytochemicals have antiplasmodial pharmacological effects, then subjected them to a stepwise in silico-based analysis, which was initiated by a comprehensive inverse docking and ended by several MDS experiments. The potential of the bioactive phytochemicals derived from the *C. aurantifolia* peels sheds light on the high capacity of waste products from edible fruits as a huge potential reservoir for health-promoting agents.

Results and discussion

Phytochemical Investigation of *Citrus aurantifolia* peels

Based on the physicochemical and chromatographic plots, the spectral investigations from UV, ^{1}H, and DEPT-Q NMR, besides correlations with the literature and some authoritative samples, the crude ethanolic extract of *C. aurantifolia* peels were found to contain the known compounds methyl isolimonate acetate 1 [29, 30], limonin 2 [31], luteolin 3 [32], 3`-hydroxygenkwanin 4 [33], myricetin 5 [34], and europetin 6 [35] (Fig. 1). The identified compound **1** was isolated herein for the first time (Figures S1-15, Fig. 1). Compound **2**, as the most active of the substances investigated in this study, was analyzed more in depth by a series of 1- and 2D NMR experiments.

Antiplasmodial activities

Malaria remains a significant public health challenge in regions of the world where it is endemic. Natural products have played a key role in the control and treatment of malaria. Quinine, a component of the bark of the *Cinchona* tree, was first used to treat malaria from as early as the 1600s and remained the mainstay for malaria treatment until the 1920s when the more effective synthetic derivative chloroquine became available [36]. Since the failure of chloroquine began in the 1960s [37], several other synthetic naturally derived compounds have been developed for clinical use including atovaquone, amodiaquine, and mefloquine [38, 39]. Since the early 2000s, the sesquiterpene lactone artemisinin, which is derived

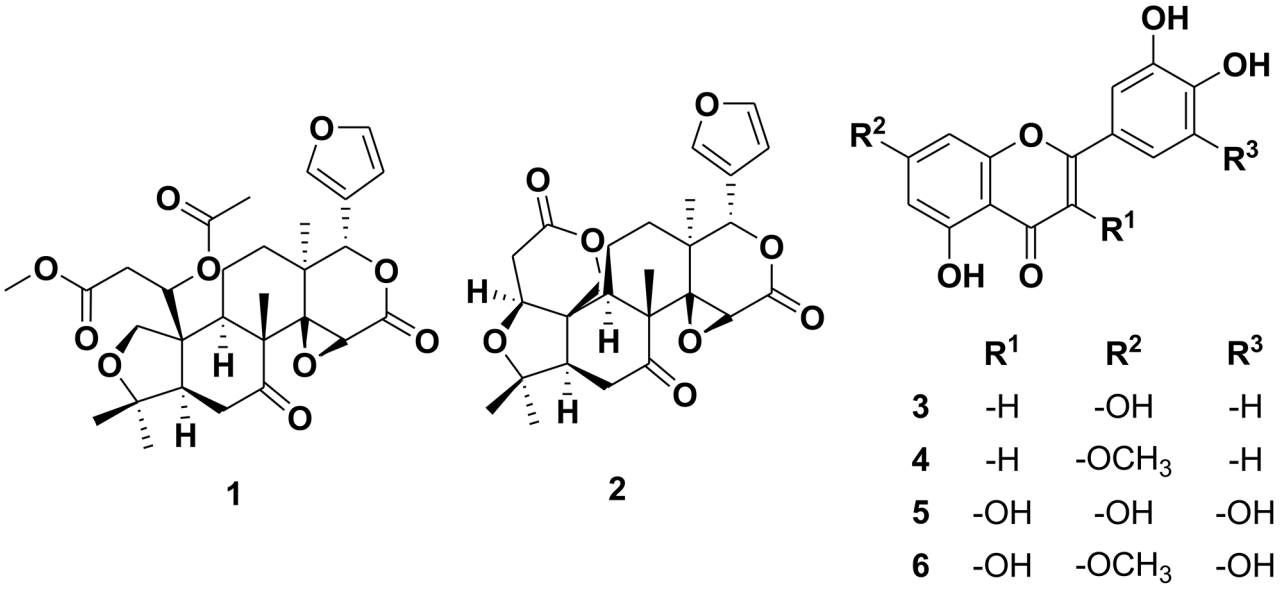

Fig. 1 Structures of compounds isolated from *Citrus aurantifolia* peels

from the sweet wormwood *Artemisia annua*, or synthetic derivatives (e.g. dihydroartemisinin, artemether and artesunate), have been used as the foundation combination drug partner in the highly effective artemisinin combination therapies. However, according to WHO, malaria is staging a comeback, in part due to the development of drug resistance. Therefore, the continued search for new anti-malarial agents remains an urgent priority.

Due to structural characteristics such as several stereocenters, flexible conformations, presence of heteroatoms, natural products are more likely than synthetic compounds to have multiple targets and/or new targets [40]. Researchers investigating natural products as potential anti-malarial drugs need to incorporate the screening of the compounds for the interaction with newly identified druggable targets, in order to identify hits/leads. Therefore, the continued exploration of natural products as antiplasmodial agents is of great scientific interest [40]. Plant-derived antiplasmodial compounds organized according to plant families covering the literature from 1990 to 2000 have been reviewed [41]. Similarly, reviews categorizing antiplasmodial compounds isolated from plants according to phytochemical classes have been conducted by Bero et al. (2005–2011) [42, 43], Nogueira and Lopes (2009–2010) [44], Tajuddeen and Van Heerden (2010–2017) [40], and Wright (2000–2010) [45]. Finally, reviews covering antiplasmodial marine natural products up to 2009 have been published by Laurent and Pietra, and Fattorusso and Taglialatela-Scafati [46, 47].

In this study, the pathogenic NF54 strain of *P. falciparum* was used to test the antiplasmodial properties of the recovered components **1**–**6** isolated from the ethanolic extract of *C. aurantifolia* peels. According to the antiplasmodial screening, the compounds limonin [2], luteolin [3], and myricetin [5] were efficacious (IC_{50} 0.2, 3.4, and 5.9 μM, respectively), while the others were inert (>50 μM).

Bioinformatics-based analysis

PPI network of the cancer related targets and KEGG-based enrichment analysis

To identify possible druggable targets for malaria disease, we first collected all previously reported malaria-derived proteins from a number of relevant databases. Using the following keywords: "malaria" and "plasmodium", we searched in the Toxicogenomics (https://ctdbase.org/) and PlasmoDB (plasmodb.org) databases, and in the the previously published literature. As a result, 3373 proteins relevant to the malaria disease were retrieved (Table S1).

To select the unique targets that are non-homolog to the human host, the collected protein targets in the previous screening were subjected to a screening based on a comparative sequence analysis (see the section Materials and methods) against the human proteome. As a result, 182 proteins (Table S2) were found to be non-homolog to the human host, and hence, they could serve as excellent candidates for in silico drug screening.

In a second step, we used the Cytoscape software to generate a protein-protein interaction (PPI) network from the 181 chosen proteins.

Figure 2 depicts the network properties of the generated PPI, which had an intermediate degree of connectivity (82 edges between 56 nodes; a mean node degree=1.05; and a local clustering coefficient value=0.281). The remaining 125 proteins in the list of

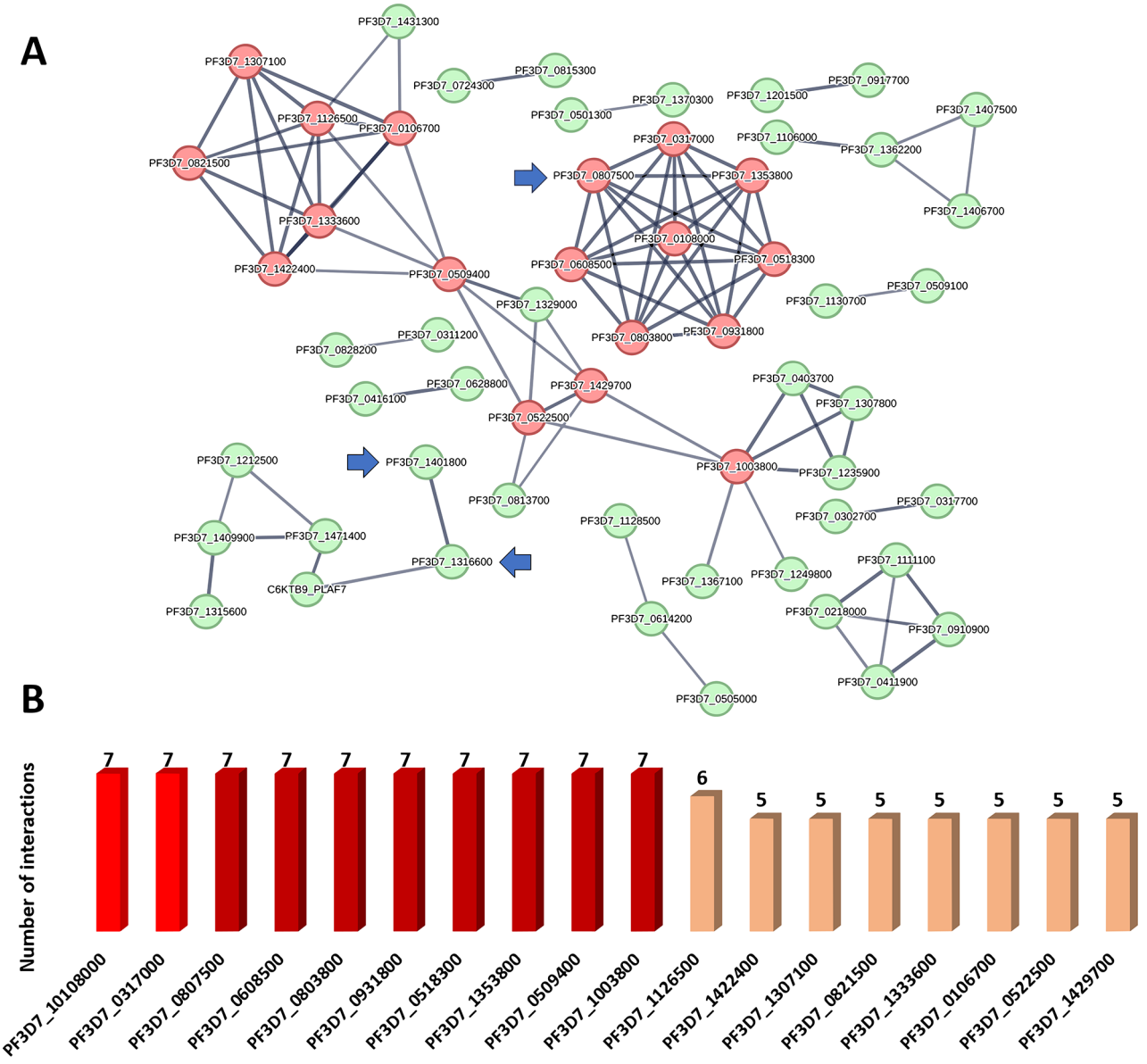

Fig. 2 (**A**): *P. falciparum* PPI network. This network consists of 56 nodes and 82 edges with an average node degree of 1.05. The top-interacting nodes are colored red (32.1%, 18 proteins of all interacting nodes, i.e., hub protein). The selection criterion for the top-interacting proteins was a minimum of five interactions for each protein. (**B**): The top interacting nodes (i.e., hub nodes arranged by their degree value). Blue arrows represent the proteins predicted as probable targets for compound **2** (limonin) investigated in the presented study. The thickness of the lines (i.e., edges) represents the degree of confidence (i.e., the strength of data support)

selected 182 proteins (Table S2) did not demonstrate any links and were thus eliminated from the PPI network.

Therapeutic strategies for diseases including malaria may have a better chance of success if they focus on proteins with high degrees of interaction, as these are typically the most important and relevant molecular targets (i.e., hub proteins or genes) in a given network [48]. Therefore, we highlighted the top 10% (i.e. 18 proteins) interacting proteins (i.e., hub proteins) in the generated network and ranked them by their degree value.

Furthermore, we classified the proteins in the current network based on their involvement in the numerous signaling pathways linked to malaria disease development. The KEGG database (https://www.genome.jp/kegg/pathway.html) was used to guide this protein enrichment analysis. Proteins presented in the PPI network (Fig. 3) were categorized according to their involvement in the key malaria disease pathways into four main groups: (i) ubiquitin–proteasome system; (ii) glycerophospholipid metabolism; (iii) DNA replication; and (iv) intracellular anatomical structure (Fig. 3). Altogether, the present

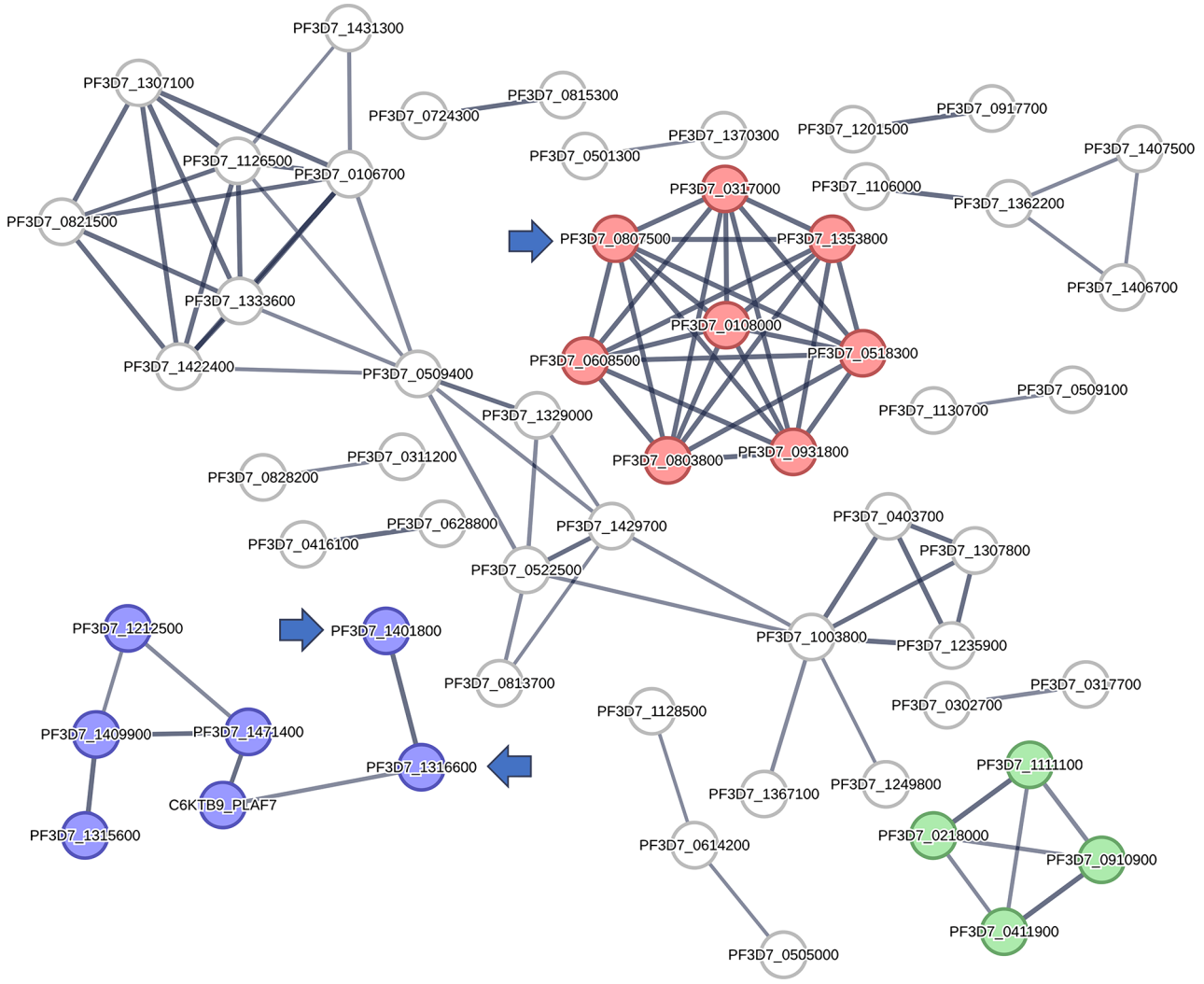

Fig. 3 The four key signaling pathways in *P. falciparum* according to the presented PPI networking. Red nodes represent the ubiquitin–proteasome system in *P. falciparum*; violet nodes exemplify the glycerophospholipid metabolism in *P. falciparum*; (iii) DNA replication in *P. falciparum*; and (iv) intracellular anatomical structure in *P. falciparum*. Blue arrows highlight the proteins predicted as probable targets for limonin (**2**) investigated in the presented study. The thickness of the lines (i.e., edges) represents the degree of confidence (i.e., the strength of data support)

protein-protein interaction (PPI) network for the disease malaria provided a brief outline of the interacting proteins and the signaling pathways associated with them, indicating the key proteins that can be considered as critical to the disease development and, thus, as good targets for drug development.

Prediction of the target proteins for the isolated compounds

Multiple in silico-based experiments were subsequently performed on compounds **1**–**6** to putatively characterize their potential as possible antiplasmodial agents. The modeled structures of compounds **1**–**6** were run through the PharmMapper (http://www.lilab-ecust.cn/pharmmapper/) prediction platform to see if they might bind to any *P. falciparum*-relevant protein target. PharmMapper is a unique pharmacophore-based virtual screening platform that can match the query structure into the 3D active sites-derived pharmacophore maps of most of the proteins hosted in the Protein Data Bank (PDB; https://www.rcsb.org/) [49]. To select potential targets for compounds **1**–**6**, we set a Fit Score of 6 as a cut-off value. Accordingly, three proteins (i.e., 7LXU, 6YXT, and 4ZCS) were predicted as potential targets for compounds **2**, **3**, and **5**, respectively, of which 7LXU had been identified as hub protein in the *P. falciparum* PPI network described above (Fig. 4). This protein is a key subunit in the 20S proteasome of *P. falciparum*, which has been found recently to be a potential target for new antiplasmodial drugs [50]. The predicted compounds (viz. **2**, **3**, and **5**) were then subjected to molecular docking and MD simulation experiments, which helped us to refine our preliminary pharmacophore-based virtual screening. Proteins

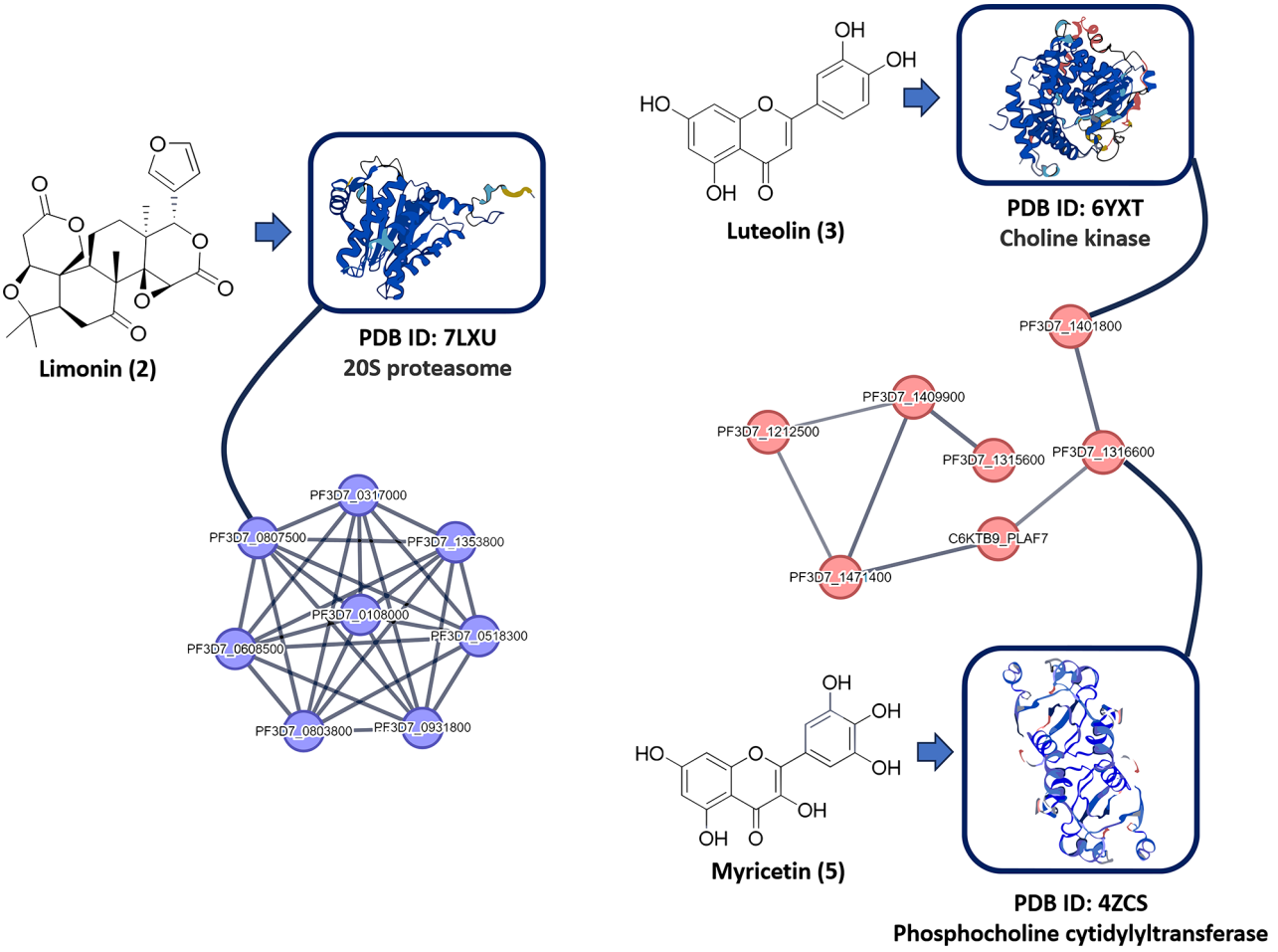

Fig. 4 Structures of the *P. falciparum*-derived proteins were predicted to be potential targets for compounds **2** (limonin), **3** (luteolin), and **5** (myricetin). Blue nodes (derived from the PPI network in Fig. 2) represent the proteasome system that limonin (**2**) was predicted to target one of its key proteins (i.e., the 20S proteasome). Red nodes represent the proteins involved in the glycerophospholipid metabolism that luteolin (**3**) and myricetin (**5**) were predicted to target two of their key proteins (choline kinase and phosphocholine cytidylyltransferase, respectively)

were candidate targets if they achieved docking scores below −7 kcal/mol and absolute binding free energies ($\Delta G_{binding}$) below −7 kcal/mol. Docking poses with scores higher than −7 kcal/mol usually are associated with low affinity in terms of $\Delta G_{binding}$ [51]. Accordingly, all the predicted proteins followed these conditions and hence, they were subjected to further refinement in 100 ns-long MD simulations.

Investigation of the modes of interaction

To investigate the binding modes of limonin (2) inside the active site of one subunit of the 20S proteasome assembly (PDB ID: 7LXU), its modeled structure was redocked into this binding site using AutoDock Vina, and then the top-scoring binding pose was inspected and subjected to a 200 ns-long MD simulation.

Limonin (2) and the co-crystallized ligand were found to share a convergent binding mode, where their interactions with the hydrophobic amino acid residues (e.g., VAL-31, LYS-33, MET-45, ALA-49, LEU-53, and CYS-159) were almost the same (Fig. 5A and B). In addition to the covalent interaction with THR-1, the co-crystallized ligand formed a single stable H-bond with GLY-47, while limonin (2) was able to maintain three stable H-bonds with THR-1, LYS-33, and SER-157. Accordingly, the binding stability of both limonin (2) and the co-crystallized ligand, were also convergent, where their RMSD profiles over the course of the MD simulation were almost identical (≈ 1.1 Å), after the first 100 ns (Fig. 5C).

In the case of both luteolin (3) and myricetin (5), each one of them was docked inside the active site of both choline kinase and phosphocholine cytidylyltransferase due to their structural similarity.

In choline kinase, both luteolin (3) and myricetin (5) first shared identical binding modes inside the active site of the enzyme, where they established multiple stable H-bonds with several amino acid residues (Fig. 6). In addition, they formed coordinates interactions with

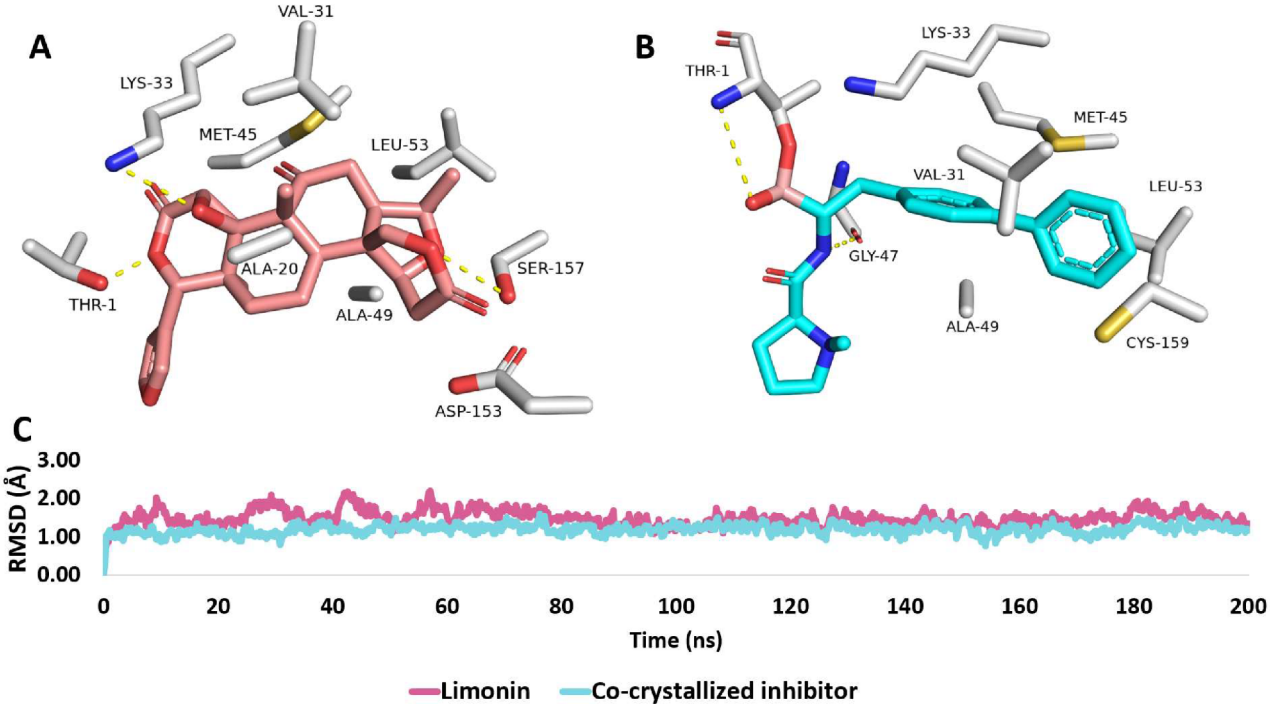

Fig. 5 (**A**) Binding modes of limonin (**2**, the brickred-colored structure) alongside (**B**) that of the co-crystallized inhibitor (cyan-colored structures) inside the active site of one subunit of the 20S proteasome assembly (PDB ID: 7LXU) of *P. falciparum* (**A** and **B**, respectively). (**C**) RMSD profiles of limonin (**2**) and the co-crystallized inhibitor over the course of 200 ns-long MD simulation

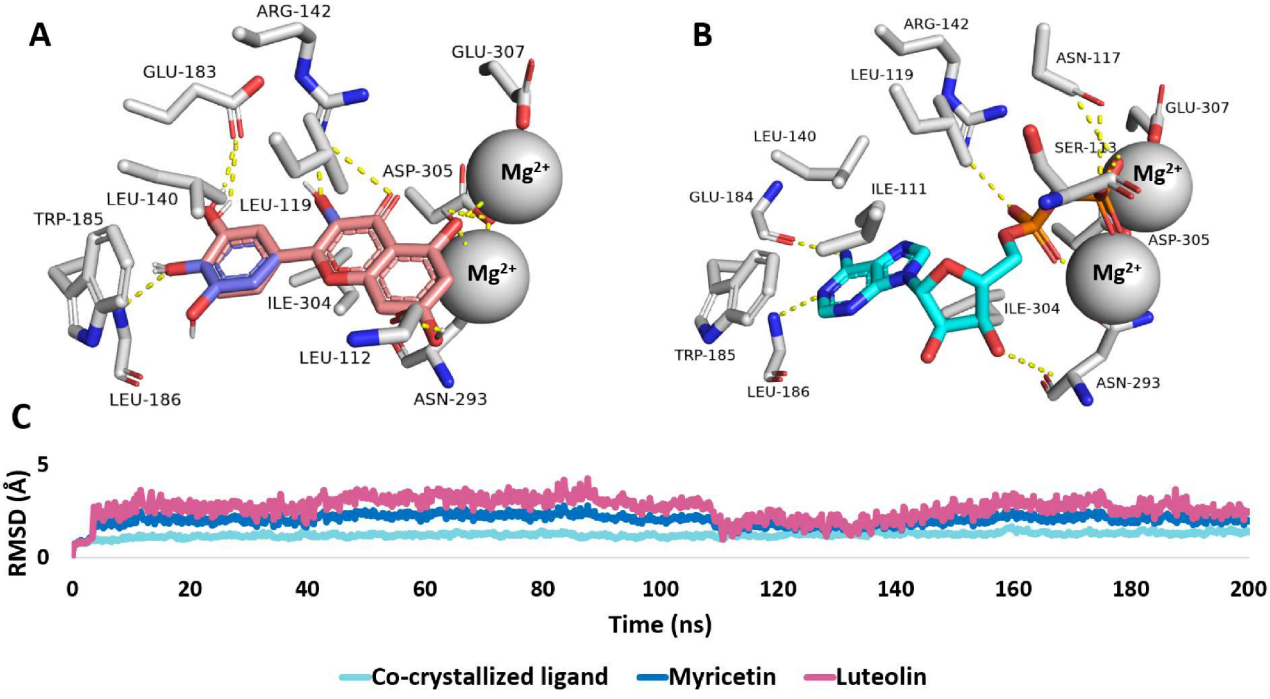

Fig. 6 Binding mode of luteolin (**3**, brickred-colored structure) in alignment with myricetin (**5**, blue-colored structures) alongside with that of the co-crystallized ligand (here ADP; cyan-colored structure) inside the choline kinase of *P. falciparum* (**A** and **B**, respectively). RMSD profiles of luteolin (**3**), myricetin (**5**), and the co-crystallized ligand over the course of 200 ns-long MD simulation

the conserved Mg^{2+}. All these hydrophilic interactions were convergent to that of the co-crystallized ligand (ADP). Accordingly, the RMSD profiles of luteolin (3) and myricetin (5) were almost identical, revealing good stability over the course of the MD simulation for both compounds **3** and **5**.

Regarding the phosphocholine cytidylyltransferase, both luteolin (3) and myricetin (5) were also identical in their binding poses and almost identical in their interactions, where myricetin (5) was able to form additional stable H-bonds with THR-753 and ASP-710. Hence, this difference was reflected clearly in their RMSD profiles, where luteolin (3) was significantly unstable inside the active site of the enzyme and was detached from it at 173 ns. The RMSD profiles of myricetin (5) and the co-crystallized ligand, by contrast, were stable, showing an average RMSD of 1.7 Å. Accordingly, these important MD simulation-based findings support only myricetin (5) to be a probable inhibitor of the phosphocholine cytidylyltransferase of *P. falciparum* (Fig. 7).

From the previous network pharmacology-based and in silico-based findings, it can be concluded that compounds **2**, **3**, and **5** are promising scaffolds for the development of novel, and efficient antiplasmodial agents that can act via multiple targets and signaling pathways. Accordingly, such a comprehensive bioinformatics-based investigation should be the first step in the development of new therapeutics, particularly from natural products.

Conclusions

Herein, we investigated the chemical composition of *Citrus aurantifolia* peels by stepwise chromatographic isolation and the subsequent spectroscopic-based structural identification, which offered six known compounds. The isolated compounds were structurally assigned and evaluated in vitro for their antiplasmodial activities against the pathogen responsible for malaria, *Plasmodium falciparum*. The results showed that only the compounds limonin (2), luteolin (3), and myricetin (5) were effective, according to their antiplasmodial activities (IC_{50} 0.2, 3.4, and 5.9 µM, respectively). We explored the antiplasmodial potential of phytochemicals from *C. aurantifolia* peels using a stepwise in silico-based analysis. We first identified the unique proteins of *P. falciparum* that have no homolog in the human proteome, and then performed inverse docking, $\Delta G_{Binding}$ calculation, and molecular dynamics simulation to predict the binding affinity and stability of the isolated compounds with these proteins. We found that limonin (2), luteolin (3), and myricetin (5) could interact with the 20S proteasome, choline kinase, and phosphocholine cytidylyltransferase, respectively, which are important enzymes for the survival and growth of the parasite. These findings suggest that phytochemicals from *C. aurantifolia* peels may have antiplasmodial activity and could be developed as safe and effective antiplasmodial compounds in the future.

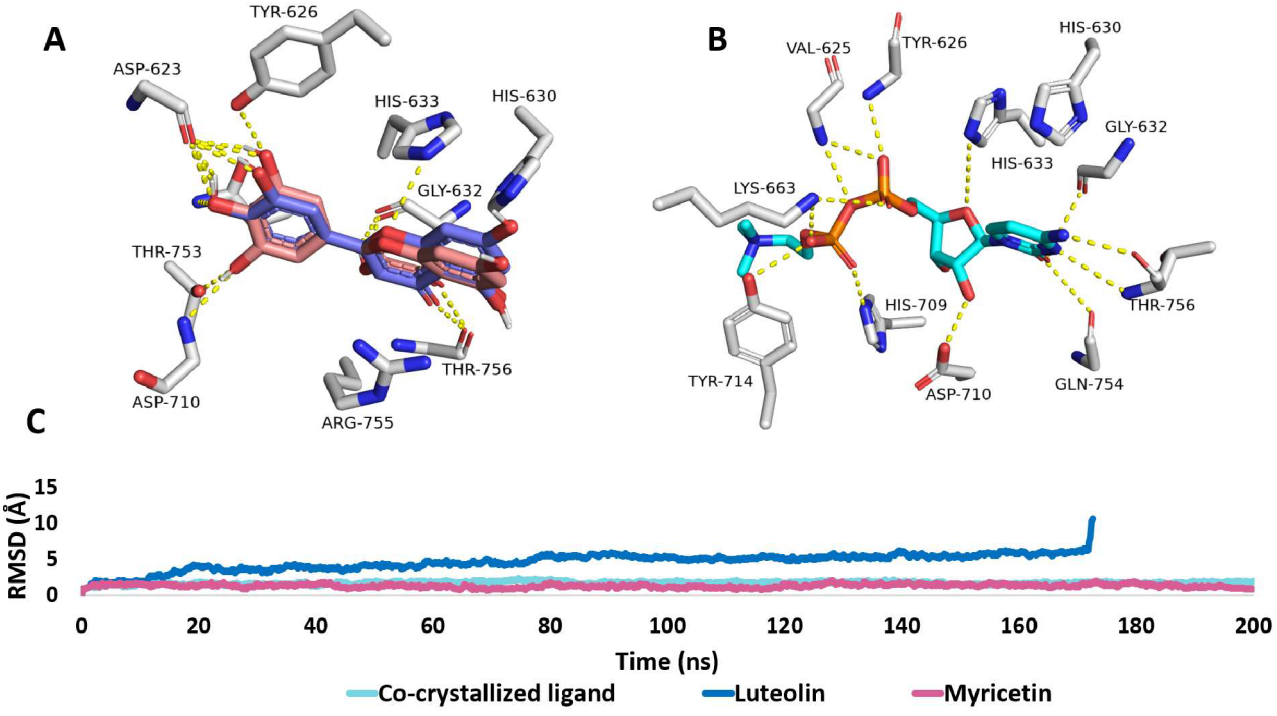

Fig. 7 Binding mode of (**A**) luteolin (**3**, blue-colored structure) in alignment with myricetin (**5**, brickred-colored structures) (**B**) alongside with that of the co-crystallized ligand (cyan-colored structure) inside the phosphocholine cytidylyltransferase of *P. falciparum* (**A** and **B**, respectively). (**C**) RMSD profiles of luteolin (3), myricetin (3), and the co-crystallized ligand over the course of 200-ns long MD simulation

Materials and methods

Plant material

Mature fruits of *C. aurantifolia* were collected in January 2021 from the House Garden, Beni-Suef, Egypt, kindly identified by Dr. Abd El-Halim A. Mohammed of the Horticultural Research Institute, Department of Flora, and Phytotaxonomy Research, Dokki, Cairo, Egypt. A voucher specimen (2021-BuPD 119) was deposited at the Department of Pharmacognosy, Faculty of Pharmacy, Beni-Suef University, Egypt.

Chemicals and reagents

The solvents used in this work included *n*-hexane (*n*-hex., boiling point b.p. 60–80 °C), dichloromethane (DCM), ethyl acetate (EtOAc), ethanol, and methanol (MeOH). They were purchased from El-Nasr Company for Pharmaceuticals and Chemicals (Egypt). Deuterated solvents used for chromatographic and spectroscopic analyses were purchased from Sigma-Aldrich (Saint Louis, Missouri, USA), including dimethyl sulfoxide-d_6 (DMSO-d_6), and chloroform-*d* ($CDCl_3$-*d*). Column chromatography (CC) was performed using silica gel 60 (63–200 µm, E. Merck, Sigma-Aldrich), while silica gel GF254 for thin-layer chromatography (TLC) (El-Nasr Company for Pharmaceuticals and Chemicals, Egypt) was employed for vacuum liquid chromatography (VLC). Thin-layer chromatography (TLC) was carried out using pre-coated silica gel 60 GF254 plates (E. Merck, Darmstadt, Germany; 20×20 cm, 0.25 mm in thickness). Spots were visualized by spraying with *para*-anisaldehyde (PAA) reagent (absolute EtOH:sulfuric acid:glacial acetic acid.:*para*-anisaldehyde (85:5:10:0.5)), followed by heating to 110 °C. luteolin (3), 3`-hydroxygenkwanin (4), myricetin (5), and europetin (6) were purchased from Sigma-Aldrich (Saint Louis, Missouri, USA).

Spectral analysis

Proton ^{1}H and Distortionless Enhancement by Polarization Transfer-Q (DEPT-Q) ^{13}C NMR spectra were recorded at 400 and 100 MHz, respectively. Tetramethyl silane (TMS) was used as an internal standard in chloroform-d ($CDCl_3$-*d*), and dimethyl sulfoxide-d_6 (DMSO-d_6), using the residual solvent peak (δ_H=7.26), and (δ_H=2.50 and δ_C=39.5) as references, respectively. Measurements were performed on a Bruker Advance III 400 MHz with BBFO Smart Probe and a Bruker 400 MHz EON Nitrogen-Free Magnet (Bruker AG, Billerica, MA, USA). Carbon multiplicities were determined using a DEPT-Q experiment, HRESIMS data were obtained using an Acquity Ultra Performance Liquid Chromatography system coupled to a Synapt G2 HDMS quadrupole time-of-flight hybrid mass spectrometer (Waters, Milford, MA, USA). In case of compound 2 the NMR spectra were recorded with a JEOL ECZ 500 (1H:500 MHz, 13C, 125 MHz) at room temperature (T = 25 °C). The ESI mass spectra was measured on an orbitrap mass spectrometer Themro Fisher Exactive driving current : 4 kV, capillary temperature: 300 °C; injection rate: 10 mL/Min. Element analysis data were determined on a HEKATech EUROEA combustionabalyzer.

Extraction and fractionation of Citrus reticulata peels

C. aurantifolia fresh peels (200 g) were finely grind using an OC-60B/60B grinding machine (60–120 mesh, Henan, Mainland China). The ground peels were extracted by maceration using 70% ethanol (300 mL, 3 × for 2 d) at room temperature, and concentrated under vacuum at 45 °C using a rotary evaporator (Buchi Rotavapor R-300, Cole-Parmer, Vernon Hills, IL, USA) to afford 40 g crude extract. The dry extract was suspended in 100 mL of distilled water (H_2O), and successively portioned with solvents of different polarities (*n*-hex., DCM). The organic phase in each step separately evaporated under reduced pressure to afford the corresponding fractions I (24.0 g) and II (5.0 g), while the remaining mother liquor was concentrated down to give the aqueous fraction (III). All resulting fractions were kept at 4 °C for biological and phytochemical investigations [52–59].

Isolation and purification of compounds

Fraction II (5 g) was subjected to normal VLC fractionation using silica gel GF_{254} (column 6×30 cm, 100 g). Elution was performed using DCM : EtOAc gradient mixtures in the order of increasing polarities (0, 5, 10, 15, 20, 25, 30, 35, 40, 45, 50, 60, 80, and 100%, 250 mL each). The effluents from the column were collected in fractions (250 mL each); and each collected fraction was concentrated and monitored by TLC using the system DCM : EtOAc=9:1, and the PAA reagent. Similar fractions were grouped and concentrated under reduced pressure to provide two sub-fractions (I_1 and I_2). Sub-fraction I_1 (1.0 g) was further fractionated on silica gel 60 (100×1 cm, 50 g). Elution was performed using a DCM : EtOAc gradient mixtures in the order of increasing polarities (0, 1, 2, 3, 4, 5, 6, 7, 8, 9, and 10%, 1 L each), to afford compound **3**, **4**, **5**, and **6** (7, 10, 13, and 16 mg, respectively). Sub-fraction I_2 (50 mg) was further fractionated on silica gel 60 (100×1 cm, 20 g). Elution was performed using DCM : EtOAc gradient mixtures in the order of increasing polarities (0, 1, 2, 3, 4, 5, 6, 7, 8, 9, and 10%, 1 L each), to afford compounds **1** and **2** (10 and 14 mg, respectively). Compound 2 was further purified on a Sephadex column with MeOH as eluent.

Antiplasmodial assay

To determine the antiplasmodial effect of isolated compounds in vitro, the Malstat assay was used as described [60]. To synchronize the culture of the *Plasmodium* NF54

strain, parasites with many ring stages were centrifuged, and the pellet was resuspended in the five-fold pellet volume of 5% w/v sorbitol /distilled H_2O and incubated for 10 min at room temperature. The cells were washed once with RPMI to remove sorbitol and further cultivated. Synchronized ring-stage parasites with 1% parasitemia of the *P. falciparum* NF54 strain were plated in triplicate in 96-well plates (200 µL/well) in the presence of a serial dilution of the extracts dissolved in 0.5% v/v dimethyl sulfoxide (DMSO). The parasites were incubated with the extracts for 72 h at 37 ˚C in the presence of nitrogen containing 5% O_2 and 5% CO_2. The incubation of parasites with DMSO at a concentration of 0.5% alone was used as a negative control, and 20% was used as a positive control. An aliquot of 20 µL was removed and added to 100 µL of the Malstat reagent (1% Triton X-100, 10 mg of L-lactate, 3.3 mg Tris and 0.33 mg of APAD (3-acetylpyridine adenine dinucleotide) dissolved in 1 mL of distilled water, pH 9.0) in a new 96-well microtiter plate. The plasmodial lactate dehydrogenase activity was then assessed by adding a 20 µL mixture of NBT (Nitro Blue Tetrazolium)/Diaphorase (1:1; 1 mg/mL stock each) to the Malstat reaction. The optical densities were measured at 630 nm, and the IC_{50} values were calculated from variable-slope sigmoidal dose–response curves using the GraphPad Prism program version 5.

Screening for the reported *P. falciparum* protein targets

Essential proteins of *P. falciparum* strain 3D7 were retrieved from GeneCards (https://www.genecards.org/) [61], Therapeutic Target Database (TTD, http://db.idrblab.net/ttd/) [62], Comparative Toxicogenomics Database (CTD, http://ctdbase.org/), and DrugBank Database (https://www.drugbank) [63]. The search was narrowed to "*Plasmodium*" and "*falciparum*". At least two-time repeating targets were chosen.

Selection of *P. Falciparum* unique proteins

Comparative sequencing analysis using the BLASTp program [64] uncovered the *P. falciparum* critical proteins that lacked a homolog in the human host proteome. In this investigation, we determined that a threshold of 35% query coverage and sequence identity was necessary for meaningful results [65]. We eliminated the proteins that shared a high degree of similarity with the human proteome and focused on the few remaining non-homologs.

Network construction, molecular docking and MD simulation

Docking was carried out using AutoDock Vina software, and MD simulations were performed with Desmond software, while the construction of PPI network was done using Cytoscape. Detailed descriptions of these procedures can be found in the Supplementary File.

Abbreviations

cMD	Classical Molecular Dynamics
DMSO	Dimethyl Sulfoxide
FEP	Free Energy Perturbation
FF14SB	Force Field 14 Stony Brook
$\Delta G_{binding}$	Absolute Binding Free Energy
GaMD	Gaussian Accelerated Molecular Dynamics
GPUs	Graphics Processing Unit
GUI	Graphical User Interface
IC_{50}	Half-maximal Inhibitory Concentration
K_i	Inhibitor Constant
MDS	Molecular Dynamics Simulation
MOI	Multiplicity of Infection
M^{pro}	Main Protease
NAMD	Nanoscale Molecular Dynamics
NIQ	Naphthylisoquinoline
NPT	Constant Pressure and Temperature
OPLS	Optimized Potentials for Liquid Simulations
PCR	Polymerase Chain Reaction
PDB	Protein Data Bank
PME	Particle Mesh Ewald
pN	Piconewton
RMSD	Root-Mean-Square Deviation
RMSF	Root-Mean-Square Fluctuation
RT	Reverse Transcriptase
RTqPCR	Quantitative Reverse Transcription Polymerase Chain Reaction
PPI	protein-protein interaction
SHAKE	Secure Hash Algorithm Keccak
SMD	Steered Molecular Dynamics
TIP3P	Transferable Intermolecular Potential with 3 Points
VMD	Visual Molecular Dynamics

Supplementary Information

The online version contains supplementary material available at https://doi.org/10.1186/s13065-024-01162-x.

Supplementary Material 1

Acknowledgements

We thank Deraya University for its laboratory facilities.

Author contributions

U.R.A. and A.H.E. Conceptualization; methodology: A.H.E., U.R.A., E.M.M., AMS, F.H.A, and G.B.; software: A.H.E., E.M.M., D.S., T.P., N.A.A., F.H.A., and G.B.; formal analysis: A.H.E., E.M.M., N.A.A., F.H.A., and G.B.; resources: A.H.E., U.R.A., D.S., T.P., N.A.A., F.H.A., and G.B.; data curation: A.H.E., U.R.A., D.S., T.P., N.A.A., F.H.A., and G.B.; writing—original draft: A.H.E. and D.S., T.P.; writing—review and editing: A.H.E., E.M.M., D.S., T.P., N.A.A., F.H.A., G.B., and U.R.A.; project administration: U.R.A.; funding acquisition: U.R.A., and N.A.A. All authors have read and agreed to the published version of the manuscript.

Funding

Open access funding provided by The Science, Technology & Innovation Funding Authority (STDF) in cooperation with The Egyptian Knowledge Bank (EKB).

Data availability

All data generated or analysed during this study are included in this published article, and its supplementary information files.

Declarations

Ethics approval and consent to participate

Not applicable.

Consent for publication

Not applicable.

Competing interests
The authors declare no competing interests.

Received: 19 October 2023 / Accepted: 8 March 2024
Published online: 30 March 2024

References

1. Kwenti TE. Malaria and HIV coinfection in sub-Saharan Africa: prevalence, impact, and treatment strategies. Research and reports in tropical medicine. 2018:123 – 36.
2. Dondorp AM, Nosten F, Yi P, Das D, Phyo AP, Tarning J, et al. Artemisinin resistance in Plasmodium Falciparum malaria. N Engl J Med. 2009;361(5):455–67.
3. Nagendrappa PB, Annamalai P, Naik M, Mahajan V, Mathur A, Susanta G, et al. A prospective comparative field study to evaluate the efficacy of a traditional plant-based malaria prophylaxis. J Intercultural Ethnopharmacol. 2017;6(1):36.
4. Newman DJ, Cragg GM. Natural products as sources of new drugs over the 30 years from 1981 to 2010. J Nat Prod. 2012;75(3):311–35.
5. Willcox ML. A clinical trial of'AM', a Ugandan herbal remedy for malaria. J Public Health. 1999;21(3):318–24.
6. Suswardany DL, Sibbritt DW, Supardi S, Pardosi JF, Chang S, Adams J. A cross-sectional analysis of traditional medicine use for malaria alongside free antimalarial drugs treatment amongst adults in high-risk malaria endemic provinces of Indonesia. PLoS ONE. 2017;12(3):e0173522.
7. Gandhi PK, Kulkarni Y. Pharamcognostical and phytochemical evaluation of three different species of citrus fruit Nimbuka, Mahalunga & Jambira (Citrus aurantifolia Linn., Citrus medica Linn., Citrus Jambiri Linn). J Pharmacognosy Phytochemistry. 2018;7(2):1192–6.
8. Elevitch C. Species profiles for Pacific Island agroforestry. Hawaii: Permanent Agriculture Resources series Western Region Sustainable Agriculture Research and Education, Holualoa; 2006.
9. Berhow MA, Bennett RD, Poling SM, Vannier S, Hidaka T, Omura M. Acylated flavonoids in callus cultures of Citrus aurantifolia. Phytochemistry. 1994;36(5):1225–7.
10. Kawaii S, Tomono Y, Katase E, Ogawa K, Yano M. Quantitation of flavonoid constituents in citrus fruits. J Agric Food Chem. 1999;47(9):3565–71.
11. Piccinelli AL, García Mesa M, Armenteros DM, Alfonso MA, Arevalo AC, Campone L, et al. HPLC-PDA-MS and NMR characterization of C-glycosyl flavones in a hydroalcoholic extract of Citrus aurantifolia leaves with antiplatelet activity. J Agric Food Chem. 2008;56(5):1574–81.
12. Peterson JJ, Beecher GR, Bhagwat SA, Dwyer JT, Gebhardt SE, Haytowitz DB, et al. Flavanones in grapefruit, lemons, and limes: a compilation and review of the data from the analytical literature. J Food Compos Anal. 2006;19:S74–80.
13. Arul D, Subramanian P. Inhibitory effect of naringenin (citrus flavonone) on N-nitrosodiethylamine induced hepatocarcinogenesis in rats. Biochem Biophys Res Commun. 2013;434(2):203–9.
14. Jayaprakasha G, Mandadi K, Poulose S, Jadegoud Y, Gowda GN, Patil BS. Novel triterpenoid from Citrus aurantium L. possesses chemopreventive properties against human colon cancer cells. Bioorg Med Chem. 2008;16(11):5939–51.
15. Poulose SM, Harris ED, Patil BS. Citrus limonoids induce apoptosis in human neuroblastoma cells and have radical scavenging activity. J Nutr. 2005;135(4):870–7.
16. Aibinu I, Adenipekun T, Adelowotan T, Ogunsanya T, Odugbemi T. Evaluation of the antimicrobial properties of different parts of Citrus aurantifolia (lime fruit) as used locally. Afr J Traditional Complement Altern Med. 2007;4(2):185.
17. Daniels S. Citrus peel extract shows benefit for diabetes. Life Sci. 2006;79:365–73.
18. Dongmo PJ, Tatsadjieu L, Sonwa ET, Kuate J, Zollo PA, Menut C. Essential oils of Citrus aurantifolia from Cameroon and their antifungal activity against Phaeoramularia Angolensis. Afr J Agric Res. 2009;4(4):354–8.
19. Souza A, Lamidi M, Ibrahim B, Aworet S, Boukandou M, Batchi B. Antihypertensive effect of an aqueous extract of Citrus aurantifolia (Rutaceae)(Christm.) Swingle, on the arterial blood pressure of mammal. Int Res Pharm Pharmacol. 2011;1(7):142–8.
20. Dongmo PMJ, Tchoumbougnang F, Boyom FF, Sonwa ET, Zollo PHA, Menut C. Antiradical, antioxidant activities and anti-inflammatory potential of the essential oils of the varieties of Citrus limon and Citrus aurantifolia growing in Cameroon. J Asian Sci Res. 2013;3(10):1046–57.
21. Yaghmaie P, Parivar K, Haftsavar M. Effects of Citrus aurantifolia peel essential oil on serum cholesterol levels in Wistar rats. 2011.
22. Abdelqader A, Qarallah B, Al-Ramamneh D, Daş G. Anthelmintic effects of citrus peels ethanolic extracts against Ascaridia galli. Vet Parasitol. 2012;188(1–2):78–84.
23. Yamada T, Hayasaka S, Shibata Y, Ojima T, Saegusa T, Gotoh T, et al. Frequency of citrus fruit intake is associated with the incidence of cardiovascular disease: the Jichi Medical School cohort study. J Epidemiol. 2011;21(3):169–75.
24. Gokulakrishnan K, Senthamilselvan P, Sivakumari V. Regenerating activity of Citrus aurantifolia on Paracetamol induced heaptic damage. Asian J Bio Sci. 2009;4(2):176–9.
25. Shalaby NM, Abd-Alla HI, Ahmed HH, Basoudan N. Protective effect of Citrus sinensis and Citrus aurantifolia against osteoporosis and their phytochemical constituents. J Med Plants Res. 2011;5(4):579–88.
26. Tosukhowong P, Yachantha C, Sasivongsbhakdi T, Ratchanon S, Chaisawasdi S, Boonla C, et al. Citraturic, alkalinizing and antioxidative effects of limeade-based regimen in nephrolithiasis patients. Urol Res. 2008;36:149–55.
27. Okon UA, Etim BN. Citrus aurantifolia impairs fertility facilitators and indices in male albino wistar rats. Int J Reprod Contracept Obstet Gynecol. 2014;3(3):640–6.
28. Effiom O, Avoaja D, Ohaeri C. Mosquito repellent activity of phytochemical extracts from peels of citrus fruit species. Global J Sci Frontier Res. 2012;12(1):1–4.
29. Bennett RD, Hasegawa S. Isolimonic acid, a new citrus limonoid. Phytochemistry. 1980;19(11):2417–9.
30. Bennett RD, Miyake M, Ozaki Y, Hasegawa S. Limonoid glucosides inCitrus aurantium. Phytochemistry. 1991;30(11):3803–5.
31. Suntar I, Khan H, Patel S, Celano R, Rastrelli L. An overview on Citrus aurantium L.: Its functions as food ingredient and therapeutic agent. Oxidative medicine and cellular longevity. 2018;2018.
32. Cuong DTD, Dat HT, Duan NT, Thuong PD, Phat NT, Tri MD, et al. Isolation and characterization of six flavonoids from the leaves of Sterculia foetida Linn. Vietnam J Chem. 2019;57(4):438–42.
33. El-Wassimy TM, Hegazy M-E, Mohamed TA, Youns SH, Al-Badry HA. Antiproliferative activity of two compounds isolated from Artemisia sieberi. J Environ Stud. 2019;19(1):14–21.
34. He D, Gu D, Huang Y, Ayupbek A, Yang Y, Aisa HA, et al. Separation and purification of phenolic acids and myricetin from black currant by high-speed countercurrent chromatography. J Liquid Chromatogr Relat Technologies®. 2009;32(20):3077–88.
35. Chung S-K, Kim Y-C, Takaya Y, Terashima K, Niwa M. Novel flavonol glycoside, 7-O-methyl mearnsitrin, from Sageretia theezans and its antioxidant effect. J Agric Food Chem. 2004;52(15):4664–8.
36. Slater AF. Chloroquine: mechanism of drug action and resistance in Plasmodium Falciparum. Pharmacol Ther. 1993;57(2–3):203–35.
37. Harinasuta T, Suntharasamai P, Viravan C. Chloroquine-resistant falciparum malaria in Thailand. Lancet. 1965:657–60.
38. Olliaro P, Mussano P. Amodiaquine for treating malaria (Cochrane Review). Cochrane Libr. 2003(4).
39. Srivastava IK, Rottenberg H, Vaidya AB. Atovaquone, a broad spectrum antiparasitic drug, collapses mitochondrial membrane potential in a malarial parasite. J Biol Chem. 1997;272(7):3961–6.
40. Tajuddeen N, Van Heerden FR. Antiplasmodial natural products: an update. Malar J. 2019;18:1–62.
41. Schwikkard S, van Heerden FR. Antimalarial activity of plant metabolites. Nat Prod Rep. 2002;19(6):675–92.
42. Bero J, Frédérich M, Quetin-Leclercq J. Antimalarial compounds isolated from plants used in traditional medicine. J Pharm Pharmacol. 2009;61(11):1401–33.
43. Bero J, Quetin-Leclercq J. Natural products published in 2009 from plants traditionally used to treat malaria. Planta Med. 2011;77(06):631–40.
44. Nogueira CR, Lopes LM. Antiplasmodial natural products. Molecules. 2011;16(3):2146–90.
45. Wright CW. Recent developments in research on terrestrial plants used for the treatment of malaria. Nat Prod Rep. 2010;27(7):961–8.
46. Laurent D, Pietra F. Antiplasmodial marine natural products in the perspective of current chemotherapy and prevention of malaria. A review. Mar Biotechnol. 2006;8:433–47.
47. Fattorusso E, Taglialatela-Scafati O. Marine antimalarials. Mar Drugs. 2009;7(2):130–52.
48. Wang T, Meng J, Zhou X, Liu Y, He Z, Han Q, et al. Reconfigurable neuromorphic memristor network for ultralow-power smart textile electronics. Nat Commun. 2022;13(1):7432.

49. Wang S, Yu M, Jiang J, Zhang W, Guo X, Chang S et al. Evidence aggregation for answer re-ranking in open-domain question answering. arXiv Preprint arXiv:171105116. 2017.
50. Xie SC, Metcalfe RD, Mizutani H, Puhalovich T, Hanssen E, Morton CJ et al. Design of proteasome inhibitors with oral efficacy in vivo against Plasmodium falciparum and selectivity over the human proteasome. Proceedings of the National Academy of Sciences. 2021;118(39):e2107213118.
51. Rastelli G, Degliesposti G, Del Rio A, Sgobba M. (2009). Binding estimation after refinement, a new automated procedure for the refinement and rescoring of docked ligands in virtual screening. *Chemical biology & drug design*, *73*(3), 283–286.
52. Al-Warhi T, Zahran EM, Selim S, Al-Sanea MM, Ghoneim MM, Maher SA. (2022) Antioxidant and wound healing potential of Vitis vinifera seeds supported by phytochemical characterization and docking studies. *Antioxidants*, *11*(5):881.
53. Elmaidomy AH, Abdelmohsen UR, Alsenani F, Aly HF, Shams SGE, Younis EA, et al. The anti-alzheimer potential of Tamarindus indica: an in vivo investigation supported by in vitro and in silico approaches. RSC Adv. 2022;12(19):11769–85.
54. Elmaidomy AH, Zahran EM, Soltane R, Alasiri A, Saber H, Ngwa CJ, et al. New halogenated compounds from Halimeda macroloba seaweed with potential inhibitory activity against malaria. Molecules. 2022;27(17):5617.
55. Bakhsh HT, Mokhtar FA, Elmaidomy AH, Aly HF, Younis EA, Alzubaidi MA, et al. Abelmoschus esculentus seed extract exhibits in Vitro and in vivo Anti-alzheimer's potential supported by Metabolomic and Computational Investigation. Plants. 2023;12(12):2382.
56. Mohamed EM, Elmaidomy H, Alaaeldin A, Alsenani R, Altemani F, Algehainy FH. Anti-alzheimer potential of a New (+)-Pinitol Glycoside isolated from Tamarindus indica pulp: in vivo and in Silico evaluations. Metabolites. 2023;13(6):732.
57. Elmaidomy AH, Mohamad SA, Abdelnaser M, Yahia R, Mokhtar FA, Alsenani F, et al. Vitis vinifera leaf extract liposomal carbopol gel preparation's potential wound healing and antibacterial benefits: in vivo, phytochemical, and computational investigation. Food Funct. 2023;14(15):7156–75.
58. Alnusaire TS, Sayed AM, Elmaidomy AH, Al-Sanea MM, Albogami S, Albqmi M, et al. An in vitro and in silico study of the enhanced antiproliferative and pro-oxidant potential of Olea europaea L. Cv. Arbosana leaf extract via elastic nanovesicles (spanlastics). Antioxidants. 2021;10(12):1860.
59. Bakhsh HT, Abdelhafez OH, Elmaidomy AH, Aly HF, Younis EA, Alzubaidi MA, et al. Anti-alzheimer potential of Solanum lycopersicum seeds: in vitro, in vivo, metabolomic, and computational investigations. Beni-Suef Univ J Basic Appl Sci. 2024;13(1):1.
60. Gamaleldin NM, Bahr HS, Mostafa YA, McAllister BF, El Zawily A, Ngwa CJ, et al. Metabolomic profiling, in Vitro Antimalarial Investigation and in Silico modeling of the Marine Actinobacterium strain Rhodococcus sp. UR111 Associated with the Soft Coral Nephthea Sp. Antibiotics. 2022;11(11):1631.
61. Rebhan M, Chalifa-Caspi V, Prilusky J, Lancet D. GeneCards: a novel functional genomics compendium with automated data mining and query reformulation support. Bioinf (Oxford England). 1998;14(8):656–64.
62. Wang Y, Zhang S, Li F, Zhou Y, Zhang Y, Wang Z, et al. Therapeutic target database 2020: enriched resource for facilitating research and early development of targeted therapeutics. Nucleic Acids Res. 2020;48(D1):D1031–41.
63. Wishart DS, Feunang YD, Guo AC, Lo EJ, Marcu A, Grant JR, et al. DrugBank 5.0: a major update to the DrugBank database for 2018. Nucleic Acids Res. 2018;46(D1):D1074–82.
64. Johnson M, Zaretskaya I, Raytselis Y, Merezhuk Y, McGinnis S, Madden TL. NCBI BLAST: a better web interface. Nucleic Acids Res. 2008;36(suppl2):W5–9.
65. Mukherjee S, Gangopadhay K, Mukherjee SB. Identification of potential new vaccine candidates in Salmonella typhi using reverse vaccinology and subtractive genomics-based approach. bioRxiv. 2019:521518.

Publisher's Note